

Localized excitons in 1D–dimensional half–filled paramagnetic Hubbard model.

N. I. Chashchin*

Ural State Forestry University

Ekaterinburg, Sibirskii trakt 37, 620100 Russia

Abstract

By the example of the Hubbard model we analytically and numerically examine the forming and coexisting of localized electron–electron pairs (doublons) and localized electron–hole pairs (Frenkel–type excitons) . Here we demonstrate that at a variation of the on-site Coulomb repulsion U there occurs a quantum transition from the doublon to the exciton regime that is conditioned by the low-energy effective hybridization of the valence and conductivity subbands. We calculate momentum distribution functions and electronic spectrum functions for different U , which reveal topologically nontrivial behaviour at the Fermi level.

Keywords: Hubbard model, electronic spectrum function, exciton, doubly occupied sites, momentum distribution function, nontrivial topology.

1. Introduction

Interplay of band theory and strong electron correlation effects has been a basic phenomenon for understanding physics of many body models and materials. Electron repulsion due to

*E-mail: nik.iv.chaschin@mail.ru

local Coulomb interactions tends to localize electrons, on the other hand, kinetic effects are favourable to electron itineracy. The energetic competition between them lead to different phases of comparable magnitude.

The single band Hubbard model (HM) [1] with one electron per site (half-filled) is the simplest model and prototypical example for investigation of correlated electrons. The initial band of noninteracting electrons is splitted into two subbands in correlated state: the lower – valence band and the upper – conductivity band. The electronic spectrum of a crystal can be organized in the form of energy bands as a function of the crystal momentum k , which is guaranteed to be a good quantum number due to the translational symmetry of the lattice. When an electron is excited from the valence into the conductivity band it leaves behind a vacancy – a hole. In a divalent crystal [2] electrons are concentrated near minimums of the conductivity band and holes near maximums of the valence band. Nearby these extremums band energy spectra in simple form are $E(k) = \hbar^2 k^2 / 2m^*$, where m^* is an effective mass of the electrons or the holes correspondingly. The vacant place (hole) in the filled valence band has the negative mass in definition, though it is convenient to consider this hole as a real particle with the positive mass and charge.

The double occupancy is a correlation function of a local pair of electrons with antiparallel spins $\langle n_{\uparrow} n_{\downarrow} \rangle$. The parameter plays an important role in the study of correlated systems, the Mott metal–insulator transition [3], the semiconductor - semimetal mixing [4], quantum phase transition [5], local moment formation, transport properties [6]. The local Coulomb repulsion disfavors doubly-occupied sites, and decreases the double occupancy [7, 8].

It is appropriate to assume that there also has to be a local bound state of an electron in the conductivity band and a hole in the valence band which are attracted to each other by the Coulomb force. The localized on a site Frenkel–type exciton $\langle (1 - n_{\sigma}) n_{\bar{\sigma}} \rangle$ is an electrically neutral quasiparticle that exists in various electronic phases of the model [9, 10, 11]. The exciton is regarded, as an elementary excitation of condensed matter, which can transport energy without transporting electric charge. The correlation effects caused by these bosonic–type single quantum states are of an interest in the study of electronic systems.

2. Theoretical Model and Method

Consider the Hubbard model in the representation we got in our previous works [12, 13, 14, 15] by using the method of generating functional of Green functions with the subsequent Legendre transformation. The Hamiltonian of the half-filled and symmetrical Hubbard model is

$$\mathcal{H} = -t \sum_{\langle i,j \rangle \sigma} c_{i\sigma}^\dagger c_{j\sigma} + \sum_{i\sigma} \varepsilon_\sigma n_{i\sigma} + U \sum_i n_{i\uparrow} n_{i\downarrow}, \quad (2.1)$$

where U is the parameter of the Coulomb interaction at a site; $c_{i\sigma}$ ($c_{i\sigma}^\dagger$) are fermion operators that describe the annihilation (generation) of electrons with spins up and down ($\sigma = \uparrow, \downarrow$); $n_{i\sigma}$ indicates the operators of the number of particles; t is the parameter of hopping of electrons from site to site; and in the designation $\langle i, j \rangle$ crystal sites are the nearest, $\varepsilon_\sigma = -\sigma \frac{h}{2} - \mu$, where $h = g\mu_B H$, g is the electron g -factor, μ_B is the Bohr magneton, H is the external magnetic field, and μ is the chemical potential.

The general equations derived in [15] are valid for different solutions — paramagnetic or magnetic. Restricting ourselves to the paramagnetic case, we get connected systems of equations for two types of Green functions.

The fermionic charge propagator ($N = 2G$)

$$N(\mathbf{k}, i\omega_n) = \frac{2}{i\omega_n - \varepsilon_k - \Sigma(\mathbf{k}, i\omega_n)}, \quad (2.2)$$

where $\varepsilon_k = -\cos(k)$ is the 1D electronic free spectrum, $\omega_n = (2n+1)\pi T$ ($n = 0, \pm 1, \pm 2, \dots$) are fermionic Matsubara frequencies, and $\Sigma(\mathbf{k}, i\omega)$ is the fermionic particle self energy.

The bosonic propagator

$$Q(\mathbf{q}, i\Omega_\nu) = -\frac{1}{1 + \frac{U}{2}\Pi(\mathbf{q}, i\Omega_\nu)}, \quad (2.3)$$

where $\Omega_\nu = 2\nu\pi T$ ($\nu = 0, \pm 1, \pm 2, \dots$) are bosonic Matsubara frequencies, and $\Pi(\mathbf{q}, i\Omega_\nu)$ is the bosonic particle self energy.

The Green function of electrons (2.2) lets the representation of the charge propagator as $N = G_- + G_+$, and the band-to-band propagator $N' = G_- - G_+$, where the indexes \pm correspond to separation of the initial electron band into the valence and conductivity subbands.

$$G_-(k, i\omega_n) = \frac{1}{i\omega_n - \varepsilon_k - \Sigma_-(k, i\omega_n)}, \quad (2.4)$$

$$G_+(k, i\omega_n) = \frac{1}{i\omega_n + \varepsilon_k - \Sigma_+(k, i\omega_n)};$$

The electronic self energy part is evaluated by the next set of equations

$$\left\{ \begin{array}{l} \Im\Sigma_+(k, \omega) = \frac{U}{4} \sum_{q'} \left[\left(1 - \tanh\left(\frac{\varepsilon_{q'}}{2T}\right) \tanh\left(\frac{\varepsilon_{q'} - \omega}{2T}\right) \right) \Im Q_-(q' - k; \varepsilon_{q'} - \omega) + \right. \\ \left. \left(1 - \tanh\left(\frac{\varepsilon_{q'}}{2T}\right) \tanh\left(\frac{\varepsilon_{k'} + \omega}{2T}\right) \right) \Im Q_+(q' - k; -\varepsilon_{k'} - \omega) \right], \\ \Re\Sigma_+(k, \omega) = \frac{1}{\pi} \int_{-\infty}^{\infty} \frac{\Im\Sigma_+(k, \omega')}{\omega' - \omega} d\omega'; \\ \Im\Sigma_+(k + \pi, \omega) = \Im\Sigma_-(k, \omega), \quad \Re\Sigma_+(k + \pi, \omega) = \Re\Sigma_-(k, \omega); \\ \Im\Sigma_+(k, -\omega) = \Im\Sigma_-(k, \omega), \quad \Re\Sigma_+(k, -\omega) = -\Re\Sigma_-(k, \omega). \end{array} \right. \quad (2.5)$$

The bosonic self energy part is evaluated by the equations

$$\left\{ \begin{array}{l} \Im\Pi_+(q, \Omega) = \frac{U}{4} \sum_{k'} \left[\left(1 - \tanh\left(\frac{\varepsilon_{k'}}{2T}\right) \tanh\left(\frac{\varepsilon_{k'} - \Omega}{2T}\right) \right) \Im G_-(k' - q; \varepsilon_{k'} - \Omega) + \right. \\ \left. \left(1 - \tanh\left(\frac{\varepsilon_{k'}}{2T}\right) \tanh\left(\frac{\varepsilon_{k'} + \Omega}{2T}\right) \right) \Im G_+(k' - q; -\varepsilon_{k'} - \Omega) \right], \\ \Re\Pi_+(q, \Omega) = \frac{1}{\pi} \int_{-\infty}^{\infty} \frac{\tanh\left(\frac{\Omega'}{2T}\right) \Im\Pi_+(q, \Omega')}{\Omega' - \Omega} d\Omega'; \\ \Im Q_+(q; \Omega) = \frac{\Im\Pi_+(q; \Omega)}{[1 + \Re\Pi_+(q; \Omega)]^2 + [\Im\Pi_+(q; \Omega) \tanh\left(\frac{\Omega}{2T}\right)]^2}; \\ \Im\Pi_+(k + \pi, \omega) = \Im\Pi_-(k, \omega), \quad \Re\Pi_+(k + \pi, \omega) = \Re\Pi_-(k, \omega); \\ \Im\Pi_+(k, -\omega) = -\Im\Pi_-(k, \omega), \quad \Re\Pi_+(k, -\omega) = \Re\Pi_-(k, \omega). \end{array} \right. \quad (2.6)$$

Thus, we get two coupled sets of the integral equations (2.5, 2.6) which can be numerically calculated and investigated. As we see, they are structurally identical over the mutual substitutions: $\Im N \leftrightarrow \Im Q$, $\Im \Sigma \leftrightarrow \Im \Pi$, and $\Re \Sigma \leftrightarrow \Re \Pi$.

The imaginary and real parts of the Green functions obey to the next symmetry properties:

$$\begin{aligned}\Im G_+(k \pm \pi, \omega) &= \Im G_-(k, \omega), & \Re G_+(k \pm \pi, \omega) &= \Re G_-(k, \omega); \\ \Im G_+(k, -\omega) &= \Im G_-(k, \omega), & \Re G_+(k, -\omega) &= -\Re G_-(k, \omega).\end{aligned}\tag{2.7}$$

3. Results and Discussion

A. Double occupancy states and local excitons

Write down the two-particle Green function in the explicit form

$$\langle \hat{T} n_{1\uparrow} n_{1\downarrow} \rangle = \langle (n_{1\uparrow} - \frac{1}{2})(n_{1\downarrow} - \frac{1}{2}) \rangle = \langle n_{1\uparrow} n_{1\downarrow} \rangle - \frac{\langle n_1 \rangle}{2} + \frac{1}{4},\tag{3.1}$$

as in our symmetrical representation $\hat{T} n_{1\sigma} = n_{1\sigma} - \frac{1}{2}$.

From the other hand [12],

$$\langle \hat{T} n_{1\uparrow} n_{1\downarrow} \rangle = \frac{1}{4} \left[\frac{\delta^2 \Phi}{\delta \rho(11) \delta \rho(11)} - \frac{\delta^2 \Phi}{\delta \eta(11) \delta \eta(11)} \right] + \frac{1}{4} \left[\left(\frac{\delta \Phi}{\delta \rho(11)} \right)^2 - \left(\frac{\delta \Phi}{\delta \eta(11)} \right)^2 \right],\tag{3.2}$$

where $\frac{\delta \Phi}{\delta \rho(11)} = \langle n_1 \rangle - 1$, $\frac{\delta \Phi}{\delta \eta(11)} = \langle n_{1\uparrow} - n_{1\downarrow} \rangle$; $\Phi = \ln Z$ is the generated functional of the connected Green functions; $1 \equiv (i, \tau)$, i -a crystal site, τ -an imaginary time; $\eta(12) = h \delta_{12}$ is the external magnetic field; $M_1 = \langle n_{1\uparrow} - n_{1\downarrow} \rangle$ - the local magnetic moment.

As we see from (3.2), determinantal factors for the propagator of double occupied sites are two-particle Green functions:

$$\langle \hat{T} M_1^2 \rangle = \frac{\delta^2 \Phi}{\delta \eta(11) \delta \eta(11)}, \quad \langle \hat{T} n_1^2 \rangle = \frac{\delta^2 \Phi}{\delta \rho(11) \delta \rho(11)}.\tag{3.3}$$

Pauli exclusion principle in the functional form [12] is

$$\frac{\delta^2 \Phi}{\delta \rho(11) \delta \rho(11)} + \frac{\delta^2 \Phi}{\delta \eta(11) \delta \eta(11)} + \left(\frac{\delta \Phi}{\delta \rho(11)} \right)^2 + \left(\frac{\delta \Phi}{\delta \eta(11)} \right)^2 = 0,$$

which allow to write (3.2) in the form

$$\langle \hat{T} n_{1\uparrow} n_{1\downarrow} \rangle = -\frac{1}{2} \frac{\delta^2 \Phi}{\delta \eta(11) \delta \eta(11)} - \frac{1}{2} (\langle M_1 \rangle)^2. \quad (3.4)$$

Comparing two expressions (3.1, 3.4) we get general formula for the number of double-occupied sites

$$\langle n_{1\uparrow} n_{1\downarrow} \rangle = \frac{\langle n_1 \rangle}{2} - \frac{1}{4} - \frac{(\langle M_1 \rangle)^2}{2} - \frac{\langle \hat{T} M_1^2 \rangle}{2}. \quad (3.5)$$

The mathematical expression for $\langle \hat{T} M^2 \rangle$ was earlier derived in [15]:

$$\begin{aligned} \langle \hat{T} M^2 \rangle &= -\frac{1}{\pi U} \sum_k \int_{-\infty}^{\infty} \tanh\left(\frac{\omega}{2T}\right) (\omega - \varepsilon(k)) \Im G_-(k, \omega) d\omega = \\ &= -\frac{1}{\pi^2 U} \int_{-1}^1 \int_{-\infty}^{\infty} \frac{d\varepsilon}{\sqrt{1-\varepsilon^2}} \tanh\left(\frac{\omega}{2T}\right) (\omega - \varepsilon) \Im G_-(\varepsilon, \omega) d\omega. \end{aligned} \quad (3.6)$$

Finally for paramagnetic $\langle M \rangle = 0$ and half-filled $\langle n \rangle = 1$ solution the average number of double-occupied sites (3.5) is

$$\langle n_{\uparrow}^e n_{\downarrow}^e \rangle = \frac{1}{4} - \frac{\langle \hat{T} M^2 \rangle}{2} \equiv \mathcal{X}(U), \quad (3.7)$$

where we denote now n_{σ}^e as the operator for electrons.

Put the next graphic designations: \circ is just a vacant place uncorrelated with other fermions, and unbound to a host-site; \ominus is a negative charged electron; \oplus is a positive charged hole.

In that case all electronic configurations on a single site can be represented in one of

particular form $\circ\circ, \overset{\uparrow}{\ominus}\overset{\uparrow}{\ominus}, \overset{\uparrow}{\ominus}\circ, \circ\overset{\uparrow}{\oplus}, \overset{\uparrow}{\ominus}\overset{\uparrow}{\oplus}, \overset{\uparrow}{\oplus}\overset{\uparrow}{\oplus}$.

Using the operator expression for a hole's number $n_{\sigma}^h = 1 - n_{\sigma}^e$ we can write the obvious identity for the average number of electrons with a certain spin direction in the system as $\langle n_{\sigma}^e \rangle = \langle n_{\sigma}^e n_{\sigma}^e \rangle + \langle n_{\sigma}^e n_{\sigma}^h \rangle$; from which we get

$$\begin{aligned} \langle n_{\sigma}^e n_{\sigma}^e \rangle &= \mathcal{X}(U) \\ \langle n_{\sigma}^e n_{\sigma}^h \rangle - \langle n_{\sigma}^e \rangle &= -\mathcal{X}(U). \end{aligned} \quad (3.8)$$

A numerical value of $\langle n_{\uparrow}^e n_{\downarrow}^h \rangle$ can be expressed in the graphic view as $\langle n_{\uparrow}^e n_{\downarrow}^h \rangle = \langle \begin{array}{c} \uparrow \\ \ominus \oplus \\ \downarrow \end{array} \rangle + \langle \begin{array}{c} \uparrow \\ \ominus \ominus \end{array} \rangle$. At that $\langle \begin{array}{c} \uparrow \\ \ominus \ominus \end{array} \rangle = \langle n_{\uparrow}^e \rangle$, and $\langle \begin{array}{c} \uparrow \\ \ominus \oplus \\ \downarrow \end{array} \rangle = \langle \mathcal{N}_{\uparrow}^{\text{exc}} \rangle$ – an excitonic pair for the single (\uparrow) spin direction. From the second equation of (3.8) we finally find the average number of localized excitons for both spin directions as

$$\langle \mathcal{N}^{\text{exc}} \rangle = -2 \mathcal{X}(U). \quad (3.9)$$

Positive or negative value of the parameter $\mathcal{X}(U)$ for different U specifies the electronic state of the system, its quantum phase. The interaction drives the bands from a semimetallic configuration to an excitonic insulating one. The excitonic nature of the new state is revealed itself in the deformed and mixed valence and conductivity subbands, which are indicating the hybridization of the original band and the correlated coexistence of electrons with holes (see Fig. 1).

B. Electronic spectra and momentum distribution function

Correlated electronic energy spectra of the conductivity $E_-(k)$ and the valence $E_+(k)$ bands as functions of the momentum k are obtained as solutions of the following electronic dispersion equations ($\Re G_{\pm}^{-1}(k, \omega + i0) = 0$):

$$\begin{aligned} E_-(k) - \varepsilon(k) - \Re \Sigma_-(k, E_-(k)) &= 0, \\ E_+(k) + \varepsilon(k) - \Re \Sigma_+(k, E_+(k)) &= 0 \end{aligned} \quad (3.10)$$

that have the following symmetry properties

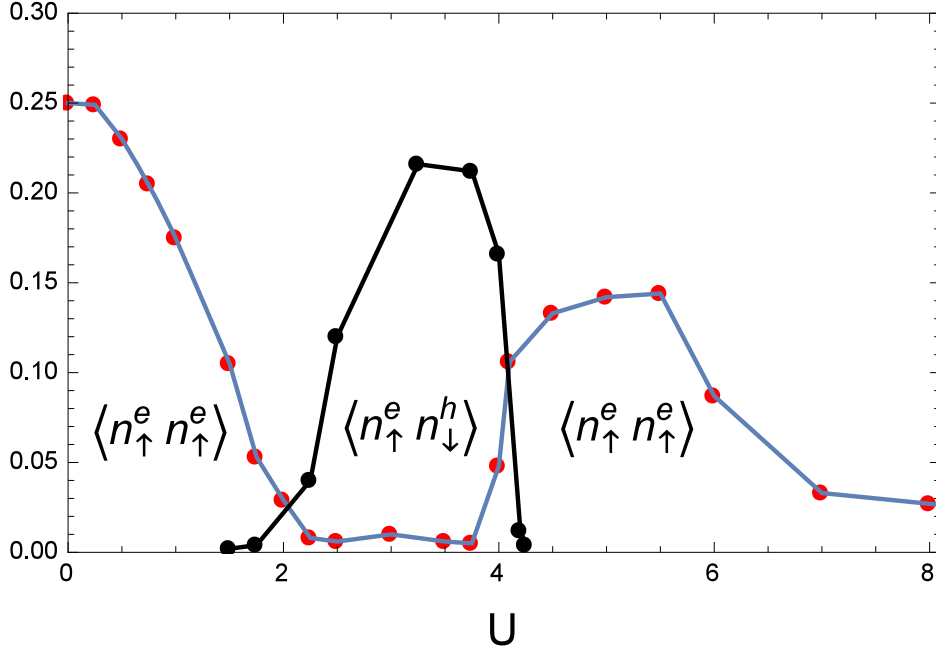
$$E_{\pm}(k) = E_{\pm}(k \pm \pi), \quad E_{\pm}(k) = E_{\mp}(k \pm \pi). \quad (3.11)$$

We calculate the behaviour of the momentum distribution function per one spin direction for the ground state of the 1D Hubbard model as

$$n(k) = \frac{1}{2} + \frac{1}{\pi} \int_{-\infty}^{\infty} \tanh\left(\frac{\omega}{2T}\right) \Im G_-(k, \omega) d\omega. \quad (3.12)$$

The momentum distribution function $n(k)$ gives an average occupation number of electronic states of the momentum k [18].

A presence or absence of a finite gap at the Fermi momentum k_F are generally considered for discerning among different sorts of an electronic behavior. The finite jump would



†

Figure 1: Double-occupied and localized excitonic sites. Here $\langle n_{\uparrow}^e n_{\downarrow}^e \rangle$ is an average number of sites with the double occupancy by electrons, $\langle n_{\uparrow}^e n_{\downarrow}^h \rangle$ is an average number of sites, which occupied by the localized excitons. The excitons are appeared and disappeared quite steeply in region $1.7 < U < 4.3$, but small amount of the double-occupancy also appear in the region. For another values of the Coulomb repulsion we observe only quite smoothly varying parameter of $\langle n_{\uparrow}^e n_{\downarrow}^e \rangle$. This situation can be considered as a sort of quantum phase transition.

indicate that the quasiparticle excitations are of the Fermi-liquid type without any gap in the spectrum and therefore, the system is of a metallic-type. For other electronic phases: insulators, semiconductors, semimetls, and excitonic insulators the function's view near the k_F considerably differs from the metallic-type behavior.

The relevance of function (3.12) refers to its analitical properties. Formally one of the deteminal factors distingwishing electronic phases of the system is an energy gap between the conductivity and the valence bands at the Fermi momentum: $\Delta = E_-(k_F) - E_+(k_F)$ which distinguish the correlated electrons from the free ones. The finite jump when $\Delta = 0$ would indicate that the quasiparticle excitations are of the Fermi-liquid type without any gap in the spectrum and therefore, the system is of a metallic-type. At $\Delta > 0$ we have an

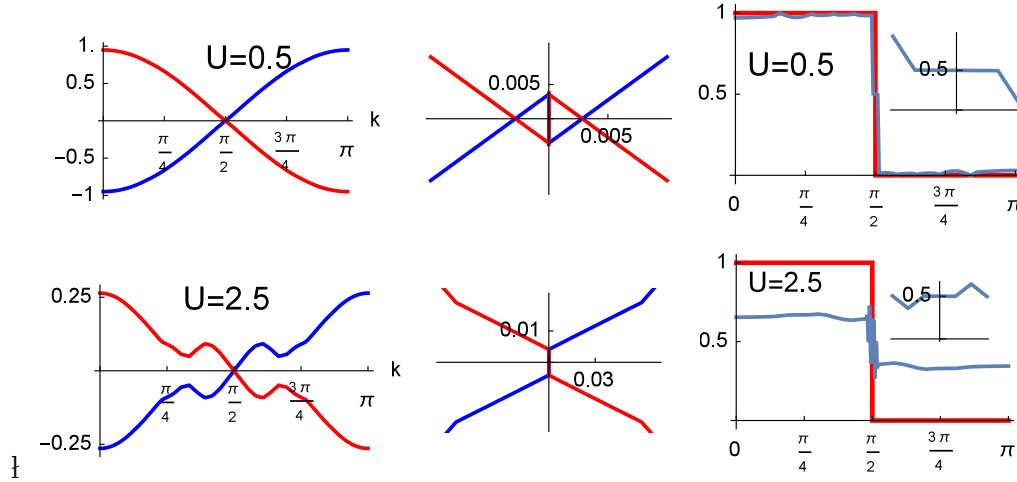


Figure 2: The top and the bottom panels are corresponding to $U = 0.5$ and $U = 2.5$. The first picture in every row represents electronic spectra $E_{\mp}(k)$, the second one is the same but near $k_F = \pi/2$; the third picture depicts the momentum distribution functions with insets for $k \approx k_F$. A flat behaviour of n_k -curve around the Fermi level demonstrates an equality of electron ($k > k_F$) and hole ($k < k_F$) numbers at the Fermi level. Note the nontrivial topology of $E_{\mp}(k)$ in the area under consideration.

insulator, when $\Delta \simeq 0$ we get a gapless semiconductor [19] and a semimetal or the excitonic insulator [10, 11] for $\Delta < 0$.

In the weak-coupling limit (small U), near the semimetal to semiconductor transition the system can become unstable against the formation of multiple excitons and this can lead to a condensation state called the excitonic insulator. Different values of band gap for $U = 0.5$ and $U = 2.5$ permit to refer the first case to the SM - phase, and the second one to EI - phase.

References

- [1] *J. Hubbard* Proc. R. Soc. A 281, 401 (1964)
- [2] *A.N.Kozlov and L.A.Maksimov* Soviet Physycs JETP, vol.21 4 (1965)
- [3] *N.F.Mott* Metal-Insulator Transitions Taylor and Francis London (1990)

- [4] *Franz X. Bronold and Holger Fehske* arXiv:cond-mat/0605415v3 [cond-mat.str-el] (2006)
- [5] *V.Yu.Irkhin and Yu.N.Skryabin* arXiv:1909.06248v1 [cond-mat.str-el] (2019)
- [6] *M.Rontani and L.J.Sham* Phys. Rev. Lett. 94 186404 (2005)
- [7] *Tudor D. Stanescu and Philip Phillips* arXiv:cond-mat/0104478v2 (2001)
- [8] *Erik G.C.P. van Loon, Friedrich Krien, Hartmut Hafermann, Evgeny A.Stepanov, Alexander I. Lichtenstein, and Mikhail I. Katsnelson* arXiv:1602.09129v1 (2016)
- [9] *N.M.Plakida* Phys.Rev.Lett. V.92 P.256401 (2011)
- [10] *B.Zenker*, arXiv:1409.2230v1 [cond-mat.str-el], (2014)
- [11] *LeeAnn M.Sager, Shiva Safaei, and David A.Mazziotti* arXiv:2002.08445v1 [cond-mat.str-el] (2020)
- [12] *Chaschin N.I.* The Physics of Metals and Metallography, vol.111 No.3 p.221 (2011)
- [13] *N.I.Chaschin* The Physics of Metals and Metallography, vol.111 No.4 p.329 (2011)
- [14] *Chaschin N.I.* The Physics of Metals and Metallography, vol.112 No.6 p.533 (2012)
- [15] *N.I.Chaschin* The Physics of Metals and Metallography, vol.117 No.7 p.663 (2016)
- [16] *Izyumov Yu.A., Chaschin N.I., Alexeev D.S., Mancini F.* Eur.Phys.J. B V.45 P.69–86 (2005)
- [17] *Chaschin N.I.*, arXiv:[707.01798v] [cond-mat.str-el], (2017)
- [18] *M.Brech, J.Voit and H. Büttner* Europhys. Lett., 12 (4) p. 289 (1990)
- [19] *I.M. Tsidilkovski* (Akademie,Berlin 1988)